Phosphatidylinositol-4-Phosphate-5-Kinase α Deficiency Alters Dynamics of Glucose-Stimulated Insulin Release to Improve Glucohomeostasis and Decrease Obesity in Mice

Ping Huang,[1,2] Oladapo Yeku,[1,3,4] Haihong Zong,[2] Phyllis Tsang,[1,2] Wenjuan Su,[1,3] Xiao Yu,[1,2] Shuzhi Teng,[6] Mary Osisami,[1,5] Yasunori Kanaho,[7] Jeffrey E. Pessin,[2] and Michael A. Frohman[1,2,3,5]

OBJECTIVE—Phosphatidylinositol-4-phosphate-5-kinase (PI4P5K) has been proposed to facilitate regulated exocytosis and specifically insulin secretion by generating phosphatidylinositol-4,5-bisphosphate (PIP_2). We sought to examine the role of the α isoform of PI4P5K in glucohomeostasis and insulin secretion.

RESEARCH DESIGN AND METHODS—The response of PI4P5Kα$^{-/-}$ mice to glucose challenge and a type 2-like diabetes-inducing high-fat diet was examined in vivo. Glucose-stimulated responses and PI4P5Kα$^{-/-}$ pancreatic islets and β-cells were characterized in culture.

RESULTS—We show that PI4P5Kα$^{-/-}$ mice exhibit increased first-phase insulin release and improved glucose clearance, and resist high-fat diet-induced development of type 2-like diabetes and obesity. PI4P5Kα$^{-/-}$ pancreatic islets cultured in vitro exhibited decreased numbers of insulin granules docked at the plasma membrane and released less insulin under quiescent conditions, but then secreted similar amounts of insulin on glucose stimulation. Stimulation-dependent PIP_2 depletion occurred on the plasma membrane of the PI4P5Kα$^{-/-}$ pancreatic β-cells, accompanied by a near-total loss of cortical F-actin, which was already decreased in the PI4P5Kα$^{-/-}$ β-cells under resting conditions.

CONCLUSIONS—Our findings suggest that PI4P5Kα plays a complex role in restricting insulin release from pancreatic β-cells through helping to maintain plasma membrane PIP_2 levels and integrity of the actin cytoskeleton under both basal and stimulatory conditions. The increased first-phase glucose-stimulated release of insulin observed on the normal diet may underlie the partial protection against the elevated serum glucose and obesity seen in type 2 diabetes-like model systems. ***Diabetes*** **60:454–463, 2011**

From the [1]Center for Developmental Genetics, Stony Brook University, Stony Brook, New York; the [2]Department of Pharmacology, Stony Brook University, Stony Brook, New York; the [3]Program in Molecular and Cellular Pharmacology, Stony Brook University, Stony Brook, New York; the [4]Medical Scientist Training Program, Stony Brook University, Stony Brook, New York; the [5]Program in Genetics, Stony Brook University, Stony Brook, New York; the [6]Department of Medical Oncology, Dana-Farber Cancer Institute, Boston, Massachusetts; and the [7]Department of Physiological Chemistry, Graduate School of Comprehensive Human Sciences and Institute of Basic Medical Sciences, University of Tsukuba, Tsukuba, Japan.

Corresponding author: Michael A. Frohman, michael@pharm.stonybrook.edu.

Received 28 April 2010 and accepted 10 November 2010.

DOI: 10.2337/db10-0614

This article contains Supplementary Data online at http://diabetes.diabetesjournals.org/lookup/suppl/doi:10.2337/db10-0614/-/DC1.

P.H. and O.Y. contributed equally to this work.

P.H. is currently affiliated with the Department of Pediatrics, Harvard Medical School, Boston, Massachusetts.

H.Z. and J.E.P. are currently affiliated with the Department of Molecular Pharmacology, Albert Einstein College of Medicine, Bronx, New York.

X.Y. is currently affiliated with the Department of Biochemistry, Indiana University, Bloomington, Indiana.

Failure of pancreatic β-cells to release adequate amounts of insulin contributes to the onset of type 2 diabetes and obesity (1). Elevated serum glucose transported into pancreatic β-cells is metabolized to increase cytosolic ATP levels, which then promote closure of ATP-sensitive K^+ (KATP) channels, causing membrane depolarization. Membrane depolarization triggers opening of L-type Ca^{2+} channels, influx of Ca^{2+}, and exocytosis. The first phase of exocytosis entails fusion of primed insulin granules predocked at the plasma membrane (2). A second phase involving mobilization of distal insulin vesicles occurs after approximately 10 min (3), preceded by actin cytoskeletal reorganization (4–6) and generation of lipid second messengers (7,8). The majority of type 2 diabetes is only weakly associated with specific genetic defects and is characterized by inadequate release of insulin, in addition to insulin resistance exhibited by fat and muscle target cells. Prolonged stimulation of β-cells by elevated levels of glucose, such as is encountered in the typical western-style high-fat diet, eventually suffices to trigger changes in insulin secretion in many individuals with otherwise seemingly normal physiology and genetics.

Lipid kinases and their phosphoinositide products play important roles in secretory vesicle trafficking (9). Type I phosphatidylinositol-4-phosphate-5-kinases (PI4P5Ks) α, β, and γ generate the signaling lipid phosphatidylinositol-4,5-bisphosphate (PIP_2). Elegant studies in neurons and neuroendocrine cells on the role of PI4P5Kγ (10,11) and PIP_2 (12–14) have revealed that PIP_2 generation at the plasma membrane is critical during regulated exocytosis. PIP_2 directly facilitates some types of Ca^{++} signaling (15,16), recruits proteins that facilitate the fusion process (13,14), and is required for docked secretory vesicles to undergo priming to become part of the ready-releasable pool and then fuse into the plasma membrane (10,11). Although less well understood mechanistically, decreased levels of PIP_2 have also been shown to inhibit insulin secretion in pancreatic β-cell model systems (7,17–19).

However, PIP_2 also carries out functions that potentially oppose regulated exocytosis (20). First, PIP_2 supports the open state of the KATP channel (21,22); thus, because it is ATP-driven closure of the KATP channel that triggers secretion, PIP_2 deficiency might be anticipated to decrease K^+ efflux, triggering membrane depolarization and thus increasing Ca^{++} currents, resulting in increased secretion (23–25). In support of this model, expression of a dominant-negative isoform of PI4P5K to lower levels of PIP_2 changes the responsiveness of mutant KATP channels with decreased

ATP sensitivity. However, expression of the dominant-negative PI4P5K does not alter function of wild-type (WT) KATP channels, suggesting that under normal physiologic conditions, the level of PIP_2 on the plasma membrane is not high enough to strongly affect KATP channel activity (26). PIP_2 has also been suggested to restrain fusion of docked vesicles by inhibiting SNARE complex function (14,27), with the restraint being alleviated through sequestration of the PIP_2 by Syntaxin-1 (14) or Ca^{2+}-triggered PIP_2 destruction (28).

Taken together, the action of PIP_2 is complex, and both its synthesis and its turnover are required at different steps in the fusion process.

Another function undertaken by PIP_2 is to promote assembly of actin filaments (F-actin) (29,30). F-actin at the periphery of the cell (cortical F-actin) has also been proposed to have both positive and negative regulatory functions in exocytosis. Cortical F-actin has been proposed to act as a barrier to block access of undocked secretory vesicles to the plasma membrane; consistent with this model, cortical F-actin is disassembled during regulatory exocytosis events (31), and pharmacologic agents that disassemble F-actin enhance movement of insulin granules to the plasma membrane and insulin release, whereas agents that stabilize the actin cytoskeleton decrease insulin release (4,18,32–34). F-actin may also affect SNARE complex function by binding to and inhibiting Syntaxin-4 function in a glucose stimulation-relieved manner (32,33). To further complicate matters, F-actin can also undertake a positive role in regulated exocytosis by mediating translocation of more internal secretory vesicles to the periphery, particularly in poorly granulated or recently degranulated cells (4,35). Thus, dynamic regulation of the actin cytoskeleton is also important in the progression of regulated exocytosis and can play positive or negative roles depending on the setting.

Changes in PIP_2 and cortical F-actin can have positive and negative effects on the secretory process, making it difficult a priori to predict the outcomes of their physiologic and experimental manipulation. Critically, individual PI4P5K isoforms may generate subpools of PIP_2 that regulate distinct components of the fusion process. Deletion of PI4P5Kγ markedly decreases levels of PIP_2 at the plasma membrane in resting neurons and neuroendocrine cells, and inhibits secretion at the stage of vesicle priming and fusion without notable effect on the actin cytoskeleton (10,11). In contrast, deletion of PI4P5Kα increases mast cell degranulation triggered by cross-linking of the IgE receptor, accompanied by minor decreases in cellular PIP_2, but significantly increased levels of Ca^{2+} signaling and decreased levels of total F-actin (36). PI4P5Kα knockdown using RNAi has also been reported to alter Ca^{2+} signaling, disrupt F-actin, and affect insulin release in a pancreatic β-cell line (37).

This report examines insulin secretion in PI4P5K$\alpha^{-/-}$ mice and finds that first-phase insulin release is augmented, and on a high-fat diet, fasting and stimulated serum insulin levels are even more elevated, conferring faster glucose clearance and resistance to the development of obesity. In this setting, K^+ and Ca^{++} signaling is seemingly normal; in contrast, the determinative factor seems to be a dramatic stimulation-dependent loss of PIP_2 at the plasma membrane that leads to reorganization of the actin cytoskeleton resulting in a near-total loss of cortical F-actin and decreased numbers of insulin granules docked at the plasma membrane.

RESEARCH DESIGN AND METHODS

Animals. PI4P5K$\alpha^{-/-}$ male mice backcrossed to C57BL/6 were genotyped per Sasaki and colleagues (36). Animal experiments were performed in accordance with the rules and regulations of the Stony Brook University Animal Care Committee. For high-fat diet, 12-week-old mice were switched from normal chow to 45% high fat (Research Diets, Inc., New Brunswick, NJ) for 8 weeks (38).

Intraperitoneal glucose and insulin tolerance tests. Mice fasted for 14 h were injected intraperitoneally with 1 g/kg 25% D-glucose in saline. Blood (5–10 μL) was collected from the tail. Blood glucose was determined by a glucometer and insulin by ELISA kit (Crystal Chem Inc., Downers Grove, IL). For insulin tolerance tests, mice were fasted for 6 h before being injected intraperitoneally with insulin (0.85 units/kg of Novolin R; Novo Nordisk, Bagsværd, Denmark). Blood glucose levels were monitored as above immediately before injection and at 15, 30, 45, 60, and 90 min after injection.

Isolation of pancreatic islets. Pancreatic tissue from 8-week-old male mice was dissolved in Hank's balanced salt solution (HBSS) containing Liberase (Roche 11815032001) and DNase I (Roche 10104159001) at 37°C for 40–50 min; digestion was stopped with HBSS/10% FBS and two washes with HBSS/2% FBS. The tissue was passed through a cell strainer and applied to a Polysucrose (Cellgrow 61196RO) gradient of 25, 23, 20, and 11% layers to isolate the islets that were aspirated from the interfaces between the 11 and 20% and the 20 and 23% gradients, washed, and picked under a dissecting microscope. Islets were used immediately or cultured in Roswell Park Memorial Institute medium/10% FBS, Pen/Strep, and glutamate.

Insulin secretion via static incubation. Pancreatic islets (n = 10) were incubated in 250 μL of Krebs-Ringer bicarbonate HEPES buffer for 30 min at 37°C, and aliquots were taken as basal samples. The glucose was increased to 20 mmol/L, and the cultures were incubated for another 30 min. Samples were placed on ice or stored at −20°C. To determine total insulin content, the islets were dissolved in 70% ethanol and 0.18 mol/L HCl overnight, sonicated, and centrifuged before samples were taken for analysis using an ultrasensitive murine insulin ELISA (Mercodia: 10115010) and BioRad plate reader. Total protein concentrations were determined with a BioRad Bradford protein assay.

Immunostaining, electron microscopy, and morphologic analysis of islets. Pancreatic islets were fixed in 4% paraformaldehyde for 20 min and permeabilized in 0.1% Triton X-100 for 20 min. Immunofluorescence staining for insulin and glucagon was performed with rabbit anti-insulin (Santa Cruz Biotechnology Inc., Santa Cruz, CA) and murine anti-glucagon (Sigma, St. Louis, MO), followed by fluorescein isothiocyanate-conjugated anti-rabbit and Alexa 546-conjugated anti-mouse antibodies (Molecular Probes, Eugene, OR). For actin cytoskeleton staining, fixed and permeabilized islets were stained with Rhodamine-phalloidin, and the fluorescence intensity was acquired from the top to the bottom of the islets using continuous xyz-scan mode on the Leica confocal microscope. All islets were scanned at the same gain intensity, and the three-dimensional series was assembled using confocal imaging software.

For electron microscopy analysis, islets were incubated in Krebs-Ringer bicarbonate HEPES buffer containing 2.8 mmol/L glucose at 37°C for 30 min (nonstimulated islets), and some were further incubated in 20 mmol/L glucose for 30 min (stimulated islets). The islets were fixed in 2% paraformaldehyde/2% electron microscopy grade glutaraldehyde in 0.1 mol/L phosphate buffer, pH 7.4 for 15 min, postfixed in 2% OsO4 in PBS for 1 h, dehydrated, infiltrated, and embedded in plastic resin. Ultra-thin sections were stained with uranyl acetate and lead citrate before examination using a FEI BioTwinG^2 transmission electron microscope (FEI Company, Hillsboro, OR). β-cell size and insulin granules were analyzed using Image J software (National Institutes of Health; http://rsb.info.nih.gov/ij/).

Statistics. Results are expressed as mean ± SD unless otherwise stated in Figs. 1–7. Statistical differences between datasets were assessed using the unpaired Student t test.

RESULTS

Enhanced insulin secretion and improved glucose tolerance in PI4P5K$\alpha^{-/-}$ mice. PI4P5K$\alpha^{-/-}$ (KO) mice fed on normal mouse chow for 8–12 weeks were visually indistinguishable from age- and sex-matched WT littermate mice but weighed significantly less (26 vs. 28 g, P = 0.03, n = 16, Fig. 1*A*). Glucose tolerance tests revealed that the fasting serum glucose levels were significantly lower in the KO mice than in the WT mice (86 ± 21 mg/dL vs. 126 ± 34 mg/dL, respectively) and that the KO mice cleared glucose faster (Fig. 1*B*). Serum insulin levels were increased in the

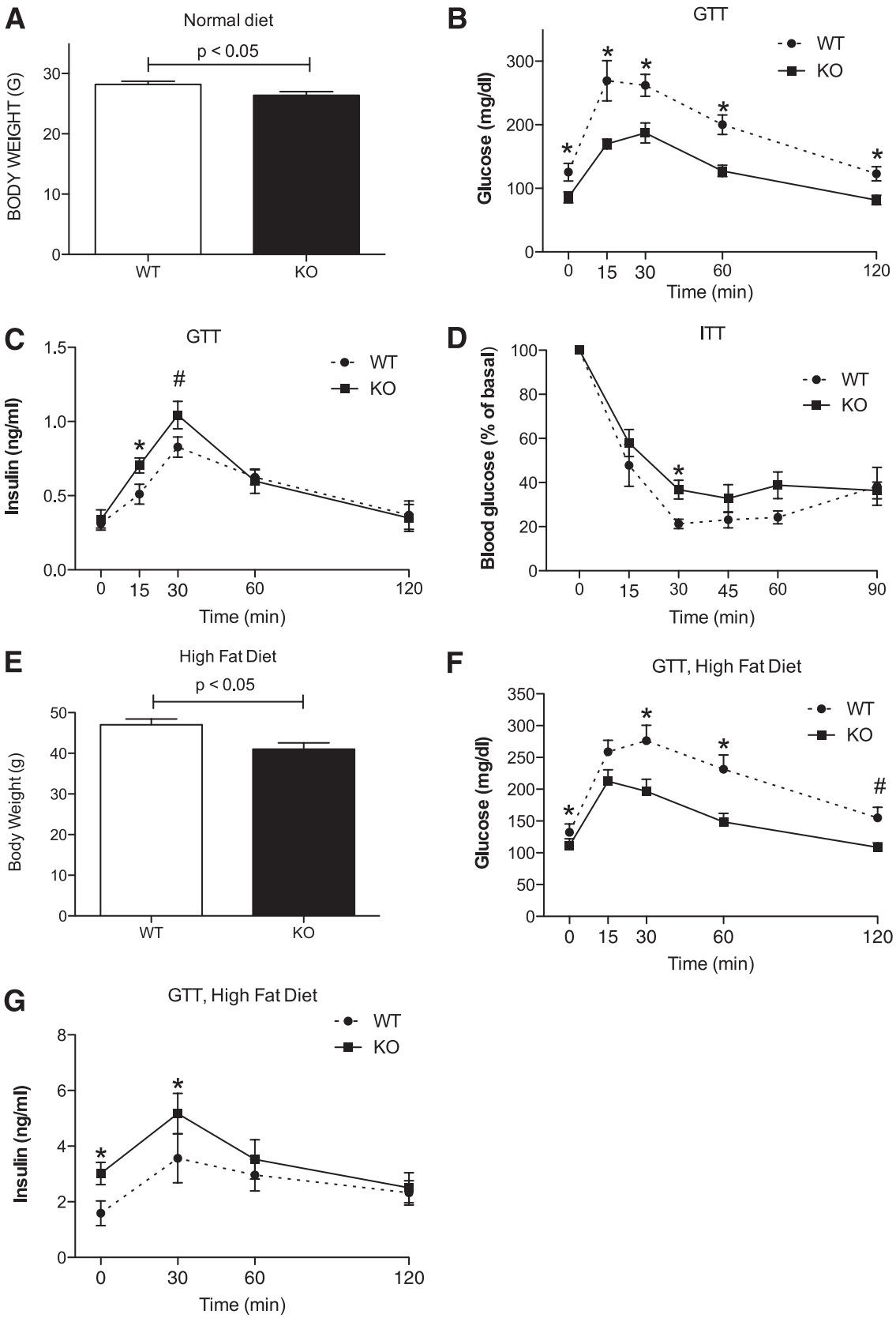

FIG. 1. PI4P5Kα KO mice exhibit improved glucohomeostasis on normal murine chow and resist development of type 2-like diabetes responses on a high-fat diet. *A*: Body weights of WT and KO mice (n = 16) raised on normal murine chow. Age-matched male mice were used for all experiments. *B*: Serum glucose levels for WT and KO mice (n = 9) in fasting mice (0 min time point) and after 1 g/kg body mass intraperitoneal injection of 25% glucose (intraperitoneal glucose tolerance test) (*P < 0.04). *C*: Serum insulin levels measured in parallel (*P < 0.05; #P < 0.1). *D*: Insulin tolerance test performed on WT and KO mice (n = 5; *P < 0.05). *E*: Body weights of WT and KO mice (n = 10) after 8 weeks on a high-fat diet. *F*: Intraperitoneal glucose tolerance test results on high-fat diet (*P < 0.03; #P < 0.06). *G*: Serum insulin levels measured in parallel (*P < 0.05, n = 7). Statistical significance determined by Student t test. Representative of three experiments. ITT, insulin tolerance test; GTT, glucose tolerance test.

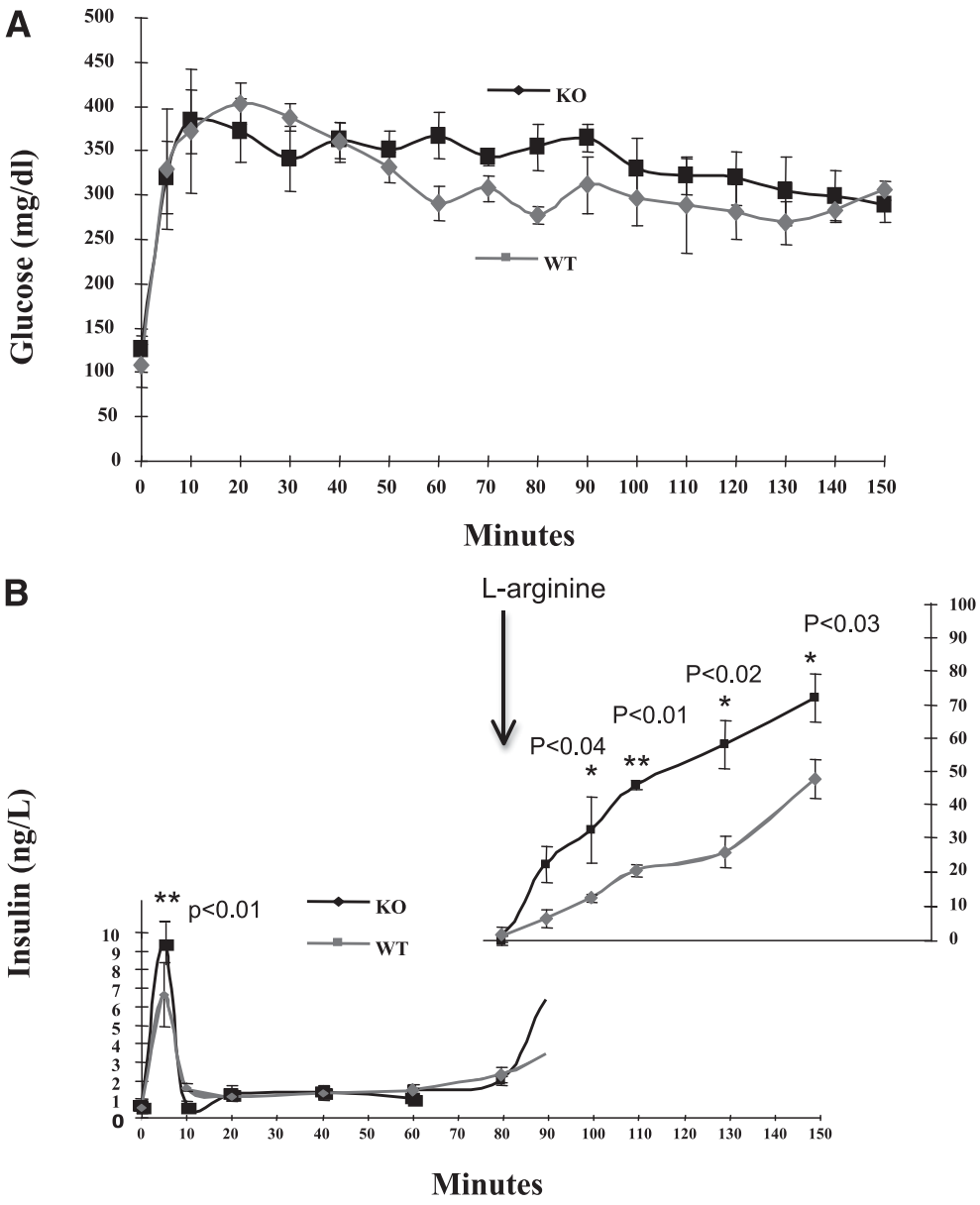

FIG. 2. First-phase GSIR and L-arginine potentiation are increased in absence of PI4P5Kα. *A*: WT and KO mice received a bolus of 20% glucose to increase serum glucose levels >250 mg/dL and were then maintained at that level by intravenous infusion adjusted for the change in serum glucose levels over time. *B*: Insulin secretion during the hyperglycemic clamp. Blood samples were taken at the intervals shown and assayed for serum insulin levels. At min 80, a bolus of 20% L-arginine and then an L-arginine infusion were added. Each experiment group was composed of four age-matched male mice. *Significant *P* values as indicated. Statistical significance determined by Student *t* test.

KO mice at 15–30' post glucose challenge (Fig. 1*C*), and total insulin secretion, calculated as area under the curve, was significantly increased ($P < 0.04$) from 67.8 ± 5.5 ng/mL/120 min to 76.2 ± 6.3 ng/mL/120 min, suggesting a basis for the improved glucose clearance. An insulin tolerance test did not reveal increased peripheral glucose utilization for PI4P5Kα KO mice in comparison with WT mice (Fig. 1*D*), ruling out the possibility of increased insulin sensitivity by target tissues as a mechanism.

PI4P5Kα KO mice resist developing type 2 diabetes-like symptoms on a high-fat diet. C57BL/6 mice placed on high-fat diets develop hyperglycemia and obesity (39). Age- and sex- matched WT and KO mice generated and maintained on the C57BL/6 background were placed on high-fat chow for 8 weeks. The mice exhibited a substantial gain in weight in comparison with mice on normal chow (Fig. 1*E* vs. Fig. 1*A*). However, the PI4P5Kα KO mice gained 30% less weight than the WT mice (Fig. 1*E*). Fasting serum glucose levels were elevated in both the WT and PI4P5Kα KO mice, although the levels remained higher in the WT mice (Fig. 1*F*). Moreover, whereas WT mice exhibited prolonged and higher elevation of serum glucose levels, the PI4P5Kα KO mice exhibited a more rapid return to euglycemia (Fig. 1*F*). Fasting and stimulated serum insulin levels were elevated in the WT mice (Fig. 1*G*). However, insulin levels in the PI4P5Kα KO mice were even further elevated under fasting (3.01 ± 0.40 vs. 1.59 ± 0.44 ng/mL for the WT mice, $P < 0.05$) and glucose-stimulated conditions.

By using the hyperglycemic clamp technique, glucose levels were clamped at ≥250 mg/dL (Fig. 2*A*) and insulin levels were measured at frequent intervals. Elevated

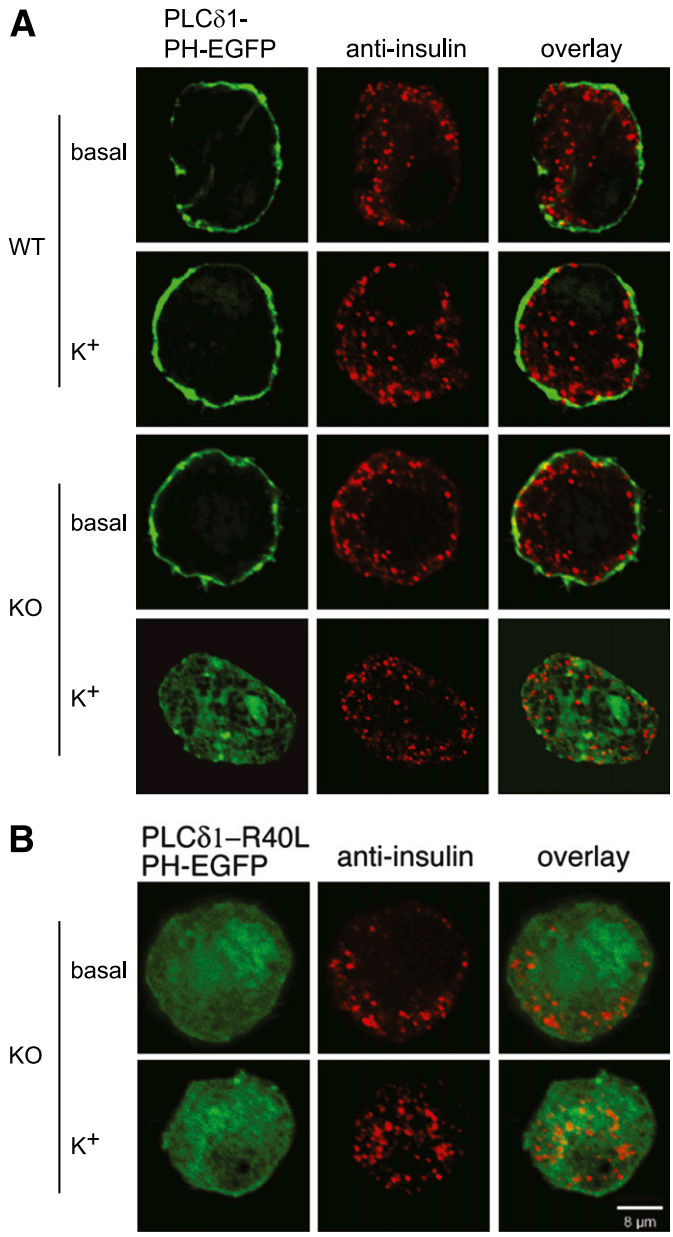

FIG. 3. Plasma membrane PIP2 is not maintained in KO β-cells on depolarization. *A*: β-cells isolated from WT and KO islets were transfected with a plasmid expressing the PIP_2 sensor PLCδ1-PH-EGFP, cultured for 2 days, depolarized with extracellular K^+ for 5 min, fixed, and imaged using confocal microscopy. Pancreatic β-cells were identified using an anti-insulin antibody in combination with a red fluorescent secondary antibody. *B*: KO β-cells expressing a mutant PIP_2 sensor (PLCδ1-PH-R40L-EGFP) that does not exhibit PIP_2 binding activity were processed as in *A*. Images were taken through the midpoints of the cells and are representative of the typical transfected, insulin-positive cells observed in the experiments ($n > 100$). The experiment was repeated at least three times using two animals each time (n = six mice), and similar outcomes were obtained. Greater than 90% of the cells examined responded as shown in the images in each condition. (A high-quality color representation of this figure is available in the online issue.)

insulin secretion ($P < 0.01$) in KO mice was observed at 5 min after the start of the glucose infusion (Fig. 2*B*), but the levels of release were subsequently similar to those of WT mice. Addition of L-arginine, a potentiator of glucose-stimulated insulin release (GSIR), resulted in increased insulin release in both WT and KO mice, but the effect was substantially greater for the KO mice.

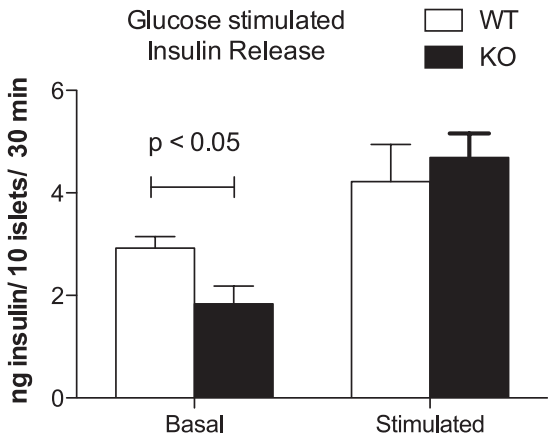

FIG. 4. PI4P5Kα KO islets secrete insulin with altered kinetics on glucose stimulation. WT and KO islets (10 islets per experimental sample, experiment performed six times) were isolated from age- and sex-matched mice, preincubated in nonstimulatory culture media (2.8 mmol/L glucose), and challenged with 20 mmol/L glucose. Six mice were used for each genotype. Incubation times were 30 min in succession for each condition. Stimulated insulin release is presented after subtraction of the basal release. Data are presented as mean ± SEM.

Taken together with the results shown in Fig. 1, these findings suggest that deletion of the *PI4P5Kα* gene results in increased first-phase glucose-dependent insulin secretion that counters the development of the type 2 diabetic-like phenotype.

Plasma membrane PIP_2 is not maintained in KO islets on stimulation. The availability of PIP_2 at the plasma membrane plays critical roles in many cell signaling processes (40). Total cellular PIP_2 levels in cells from PI4P5Kα KO mice were examined previously (36) and found to be decreased only modestly (90% of WT levels). However, PIP_2 exhibits rapid turnover and resynthesis at the plasma membrane on glucose-triggered β-cell stimulation as a consequence of Ca^{2+}-mediated phospholipase C activation (28). The signaling pathway leading to PIP_2 turnover can also be initiated by elevating levels of extracellular K^+ to depolarize the β-cell, thereby triggering the same downstream effects (18). We used this approach to examine whether there were differences in basal or stimulated levels of accessible PIP_2 at the plasma membrane of isolated pancreatic β-cells as reported by a fluorescent PIP_2 sensor based on fusion of EGFP to the PIP_2-binding PH domain of PLCδ1 (PLCδ1-PH-EGFP). Primary pancreatic β-cells were transfected in vitro with a reporter plasmid expressing PLCδ1-PH-EGFP, with a transfection frequency of 80–85% (Supplementary Fig. 1). Under basal conditions, PIP_2 was readily imaged at the plasma membrane in both the WT and KO cells (Fig. 3*A*, *rows 1 and 3*), although it should be noted that this observation demonstrates only that the minimal threshold for sensor recruitment is in place, not necessarily that the levels of accessible plasma membrane PIP_2 are quantitatively identical. However, differences were observed on K^+-elicited depolarization. Whereas no change was observed for WT β-cells, indicating that the rates of resynthesis of PIP_2 compensated for the depolarization-triggered turnover, relocalization of the sensor from the plasma membrane to the cytoplasm was observed for the PI4P5Kα KO cells. A mutant sensor, PLCδ1-R40L-PH-EGFP, which lacks the capability to bind PIP_2, distributed uniformly in the cytoplasm under both basal and stimulated conditions (Fig. 3*B*). There were no obvious changes in localization of the insulin

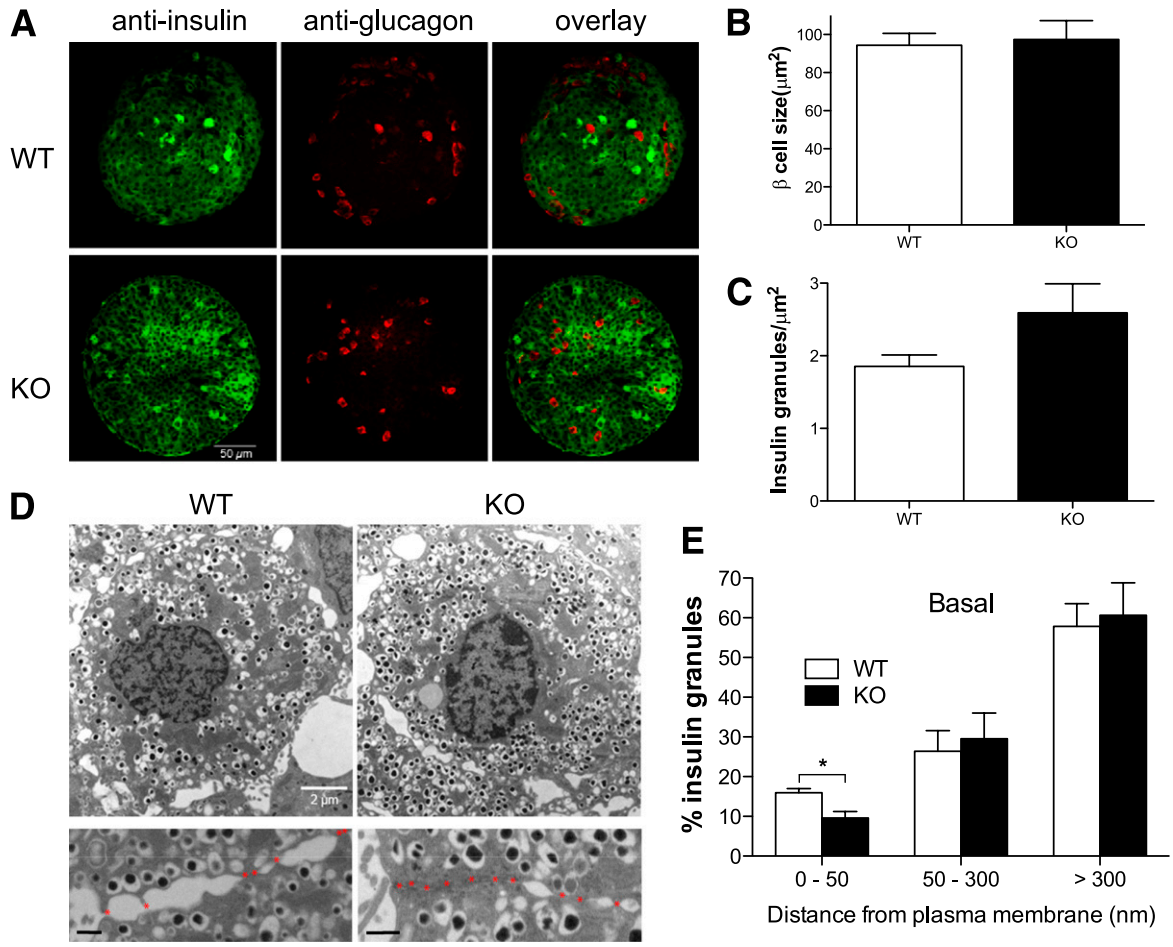

FIG. 5. Morphology of islets, β-cell size, and insulin granule density are not noticeably different in PI4P5Kα KO mice, but distance of granules from cortex is. *A*: Confocal microscopy image of WT and KO islets stained with anti-insulin and antiglucagon primary antibodies to visualize β-cells and α-cells, respectively. *B*: Quantitation of WT and KO β-cell size using transmission electron microscopy. *C*: Quantitation of the number of insulin granules contained in WT and KO islets normalized for the size of the each islet. *D*: Transmission electron microscopy images of WT and KO islets. KO β-cells show less insulin vesicles docked at the plasma membrane in comparison with WT β-cells (magnified lower panels; bar, 500 nm). Asterisks indicate boundaries between adjacent β-cells. *E*: Distance of subgranular pools of insulin to the plasma membrane in WT and KO cells under basal conditions. Insulin granules were grouped into three categories with respect to distance from plasma membrane: <50, 50–300, and >300 nm. Granules located with 50 nm from plasma membrane were considered to be docked granules. Granules were tabulated from 10 sections for each genotype. Data are presented as mean ± SEM. (A high-quality color representation of this figure is available in the online issue.)

granules in the isolated PI4P5Kα KO cells under basal or stimulated conditions in comparison with the WT cells.

These results indicate that plasma membrane PIP_2 decreases after depolarization (stimulation) of the PI4P5Kα KO β-cells, but because of a reduced capacity for resynthesis, the recovery of PIP_2 levels at the plasma membrane is blunted.

PI4P5Kα KO islets exhibit alterations in ex vivo insulin secretion. Surprisingly, release of insulin by PI4P5Kα KO islets cultured ex vivo was significantly less under basal conditions, but similar to WT on glucose stimulation (Fig. 4). We measured the total insulin content per islet (112 ng/islet, WT, vs. 94 ng/islet, KO; NS), examined islet appearance using anti-insulin and glucagon immunostaining to visualize β- and α-cells, respectively (Fig. 5*A*), and examined β-cell morphology by electron microscopy (Fig. 5*D*) to estimate β-cell size (Fig. 5*B*) and the number of insulin granules per cell (Fig. 5*C*). No significant differences were found between the WT and PI4P5Kα KO islets for any of these parameters. We also used quantitative RT-PCR to examine expression levels for the other two PI4P5K isoforms, β and γ, but did not observe compensatory upregulation (Supplementary Fig. 2). However, quantitative analysis of the subcellular distribution of insulin granules by electron microscopy (41,42) revealed that decreased numbers of granules were docked at the plasma membrane in the PI4P5Kα KO cells (i.e., were localized within 50 nm of the plasma membrane) (Fig. 5*D* and *E*), suggesting a basis for the decrease in basal insulin secretion in KO mice in the ex vivo experiments. On glucose stimulation, the number of granules localized at 50–300 nm from the plasma membrane decreased in both WT and KO β-cells, whereas the number of granules localized within 50 nm of the plasma membrane increased; no significant differences were seen at that point between WT and KO β-cells for insulin granule distribution within 50 nm of the plasma membrane, indicating that the readily releasable pool was rapidly replenished once the glucose stimulatory pathway had been activated.

WT and KO islets exhibit comparable K^+ and Ca^{++} signaling on β-cell stimulation. Key steps in the glucose-stimulated insulin secretion pathway involve KATP channel closing and membrane depolarization that triggers increased intracellular Ca^{2+}, and disassembly of cortical F-actin, all of which could be regulated by PIP_2 availability. To examine

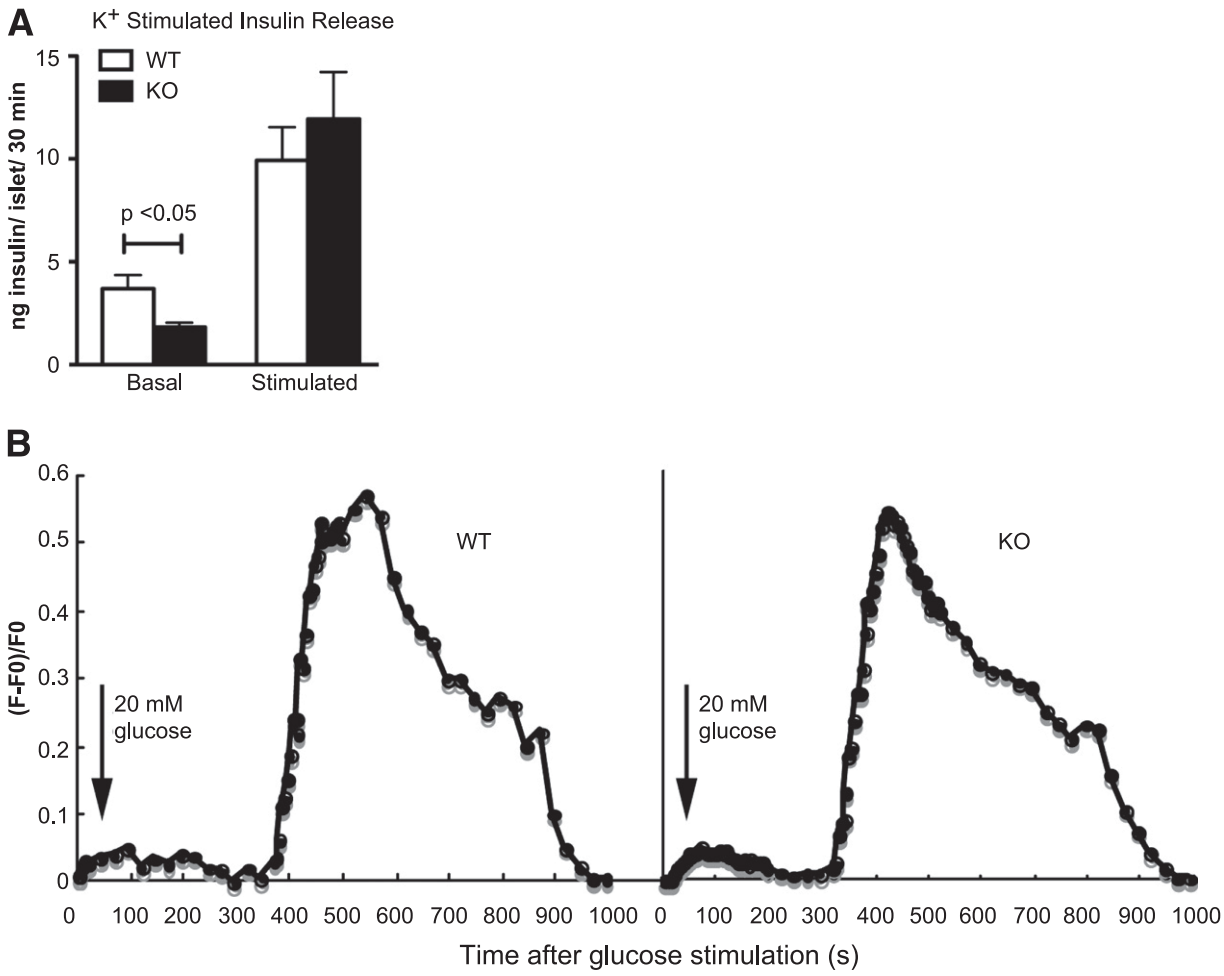

FIG. 6. PI4P5Kα KO islets secrete insulin with altered kinetics on K^+ depolarization and display comparable Ca^{2+} influx on glucose stimulation. *A*: WT and KO islets (10 islets per experimental sample, experiment was performed nine times) were isolated from age- and sex-matched mice, preincubated in nonstimulatory culture media (2.8 mmol/L glucose), and challenged with 60 mmol/L K^+. Incubation times were 30 min in succession for each condition. Stimulated insulin release is presented after subtraction of the basal release. Data are presented as mean ± SEM. *B*: Ca^{2+} influx was measured by fluorescent quantification in WT and KO islets before and after glucose stimulation. The cytosolic Ca^{2+} concentration was measured using Fluo-4 dye, and the relative intensity change (F-F0)/F0 vs. time was plotted, where F0 and F stand for resting fluorescence and fluorescence after 20 mmol/L glucose stimulation, respectively. Traces of individual islets representative of three experiments are shown.

whether differences in KATP channel closing differentially triggered insulin secretion, we bypassed the channel closing step using elevated extracellular K^+ to directly depolarize the cells. As with glucose stimulation, the PI4P5Kα KO islets exhibited lower levels of insulin release under basal conditions, and then levels of release on depolarization that were similar to that observed for the WT islets (Fig. 6*A*). We also performed patch clamping on isolated β-cells to examine KATP channel inactivation, but no differences were noted between WT and PI4P5Kα KO cells (data not shown). These results suggested that the step affected by the loss of PI4P5Kα-generated PIP_2 lies downstream of KATP channel depolarization. We next measured intracellular Ca^{2+} levels in both WT and KO islets on glucose stimulation, but did not observe significant differences between the genotypes on glucose stimulation (Fig. 6*B*). Taken together, these findings indicate that the metabolic signaling pathway that proceeds from glucose import to increased intracellular Ca^{2+} is normal in PI4P5Kα KO β-cells.

F-actin organization is diminished at the cell cortex membrane of PI4P5Kα KO islets. Under basal conditions, most of the F-actin in WT β-cells localized to the plasma membrane (Fig. 7*A*). However, in PI4P5Kα KO β-cells, the amount of cortical F-actin was greatly diminished, with much of the residual fluorescence appearing diffuse or relocalized to internal sites suggestive of vesicles or stress fibers (Fig. 7*A*). On glucose stimulation for 5 min, much of the cortical F-actin in the WT β-cells was disassembled, with relocalization to stress fibers noted in some cells (Fig. 7*B*); in contrast, F-actin was virtually completely absent in glucose-stimulated PI4P5Kα KO β-cells. Quantitation of the F-actin fluorescence revealed a 60% decrease in the PI4P5Kα KO cells in comparison with WT islets under basal conditions and an 80% decrease after stimulation with glucose for 5 min (Fig. 7*C*). No difference in total actin in the KO cells was observed (Fig. 7*D*).

DISCUSSION

Both positive and negative roles have been described for PIP_2 and the actin-cytoskeleton network in regulation of exocytosis and in particular insulin secretion. PIP_2 is required for vesicle fusion at the plasma membrane (10,11), but also inhibits SNARE complex-mediated fusion (14) and facilitates KATP channel activity (21–23), which opposes

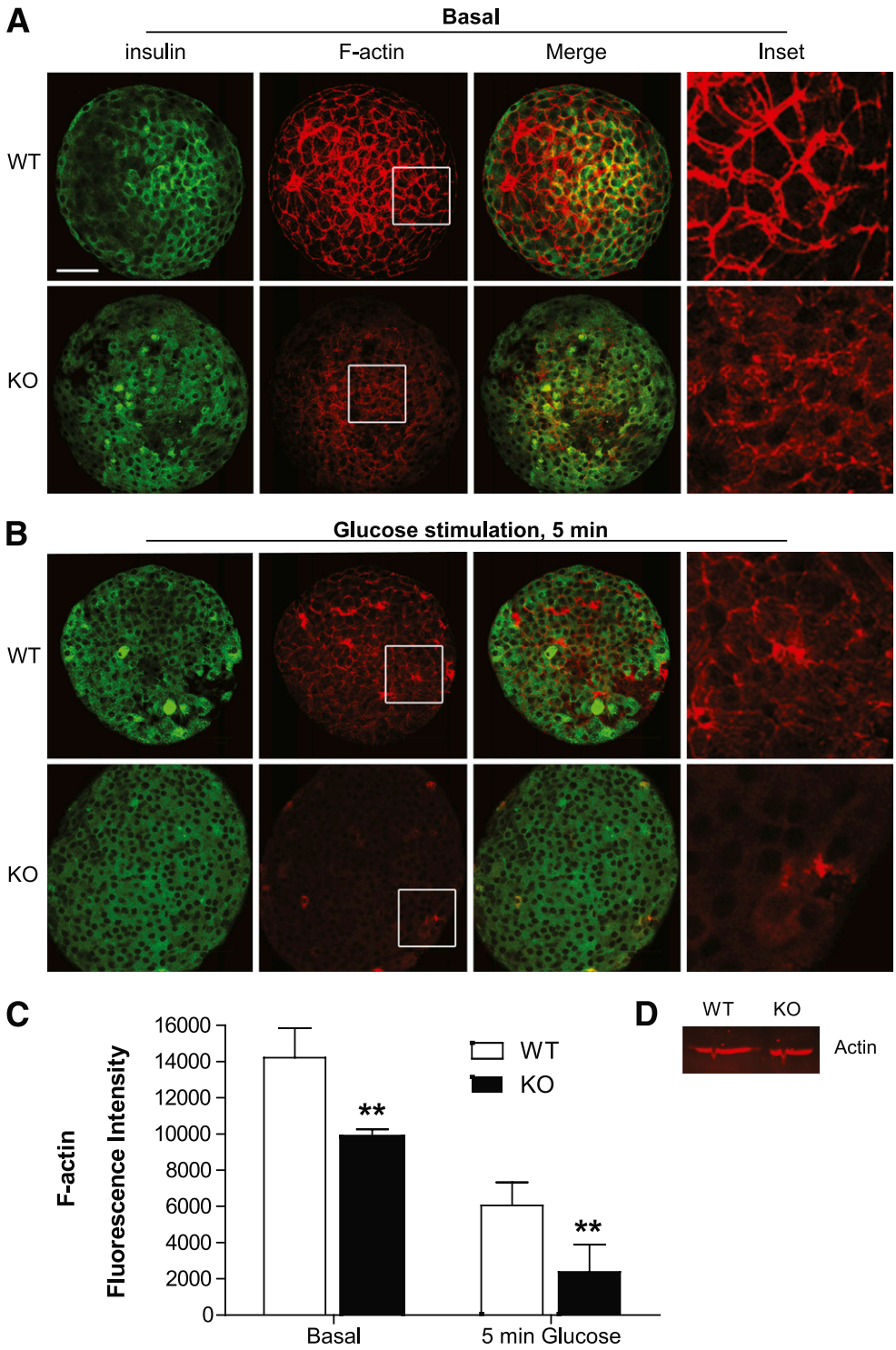

FIG. 7. PI4P5Kα KO islets exhibit a dramatic deficiency in cortical F-actin under both basal and stimulated conditions. WT and KO islets were stained for F-actin using rhodamine-phalloidin before (*A*) and after (*B*) glucose stimulation for 5 min and fixation. Pancreatic β-cells were visualized using anti-insulin primary antibody with confocal microscopy. Shown are individual optical sections. Compiled sets of the optical sections are presented in the Supplementary Data. Scare bar, 50 μm. *C*: Quantification of F-actin fluorescence. Fluorescence intensity was acquired from the top to the bottom of the islets using continuous xyz-scan mode on the Leica confocal microscope. All islets were scanned at the same gain intensity, and the three-dimensional series was assembled using the confocal imaging software. Total fluorescence intensity was determined for 10 islets, and average fluorescence and standard deviation were determined. **$P < 0.01$. *D*: Western blot for actin from lysates of WT and KO cells, representative of four experiments. (A high-quality color representation of this figure is available in the online issue.)

insulin release. Cortical F-actin serves as a barrier that prevents secretory vesicle access to the plasma membrane (18,31,43) and inhibits SNARE complex-mediated fusion (33), but it also promotes movement of secretory granules to the plasma membrane from regions deeper in the cell (4). In summary, both turnover (14,18,20,28) and synthesis (7,10,11,13,14,17–19) of PIP_2 are required at different steps in the secretory process, and dynamic reorganization of

the actin cytoskeleton is also important (4,32,34,35). One way that this is achieved is through the use of different PIPK isoforms; PI4P5Kγ and the type 2 PIP_2-synthesizing enzyme, PI5P4Kβ, generate a pool of PIP_2 required for vesicle fusion in neurons and pancreatic β-cells (7,10,11,19) that does not substantially regulate the actin cytoskeleton. In contrast, PI4P5Kα appears to generate a pool of PIP_2 that inhibits exocytosis in mast cells, potentially through stabilizing F-actin (36). Plasma membrane PIP_2 exists in microdomains, some of which colocalize with syntaxin and promotes exocytosis (44), and others which colocalize with lipid rafts and regulate cortical actin assembly (44,45). PI5P4Kβ colocalizes with and regulates the syntaxin-associated PIP_2 microdomains (44); it is possible that PI4P5Kα may localize and regulate the lipid-raft associated PIP_2 microdomains.

This study reports alterations in insulin release by pancreatic β-cells in mice lacking PI4P5Kα. The KO mice exhibit increased first-phase insulin secretion and improved glucose clearance under normal diet chow, and elevated insulin under fasting and GSIR conditions on a high-fat diet. Changes in K^+ and Ca^{++} signaling were not observed, which is consistent with the report that under normal physiologic conditions, the level of PIP_2 on the plasma membrane is not high enough to strongly affect KATP channel activity (26), and thus decreasing it via ablation of PI4P5Kα has no effect on glucose-stimulated changes in K^+ currents. In contrast, a dramatic decrease of cortical F-actin was observed, accompanied by decreased numbers of insulin granules docked at the plasma membrane and less insulin secretion under basal ex vivo conditions.

Unexpectedly differing results were observed between the in vivo and ex vivo GSIR model systems. Multiple reasons may underlie the findings, but we would suggest that differences in the assay conditions could be the major factor. Normal physiology involves serum glucose levels in mice of ~120 mg/dL, or 6.6 mmol/L glucose, which is a modestly stimulatory level under ex vivo conditions. In the ex vivo assay, however, islets were placed in low glucose, 2.8 mmol/L, or ~50 mg/dL, a nonstimulatory condition, before assaying basal insulin release. It is likely that under "basal" conditions in vivo (6.6 mmol/L glucose), a low chronic level of β-cell stimulation leads to continued transport of insulin granules to the plasma membrane. In pancreatic β-cells from PI4P5Kα KO mice with diminished cortical F-actin, the barriers to fusion are decreased, and exocytosis rapidly occurs, leading to elevated insulin release, sustained by the continued replacement of the granules via microtubule transport. This low-level, chronic release of insulin on ad lib normal chow could account for the decreased serum glucose levels observed, although insulin levels were not significantly increased under fasting conditions. Under high-fat diet conditions, insulin levels were increased under fasting conditions in mutants, presumably reflecting the elevated serum glucose that provides a greater chronic stimulation to the β-cells. In the ex vivo setting (2.8 mmol/L), however, the lower level of β-cell stimulation may fail to suffice to promote the granule transport, leading to decreased release once the cortical population of granules has been sufficiently diminished, as suggested by our morphologic analysis. On elevated glucose stimulation, however, transport resumes, leading to similar levels of insulin release as barriers to fusion are decreased in the WT pancreatic β-cells as well. The increased first-phase in vivo release may also suggest that granule transport to the plasma membrane or some other step in the distal part of the process is facilitated in the KO cells.

Regardless of the precise mechanistic relationship between insulin secretion and cortical F-actin, the relatively subtle changes in insulin secretion seem to have a substantial effect on the obesity and hyperglycemia in the C57BL/6 high-fat animal model. We would suggest that the elevated first-phase release of insulin leads to a more rapid return to euglycemia under conditions of exaggerated nutrient uptake, decreasing the prolonged stimulation of β-cells that is associated with eventual aberrant signaling, blunted insulin release, and cell death. It should be noted that glucose homeostasis is a complex physiologic process. β-cells and GSIR play a central role in the process, but other hormones and the liver, muscle, and adipose tissue are also involved. It is possible that some of these other physiologic processes might contribute to the phenotype we observed. High-fat murine models are not necessarily predictive of outcomes for type 2 diabetes in humans, but this work suggests the idea that development of therapeutics that increase early release of insulin as described in this report might be valuable as adjuncts for current therapies targeted toward increasing insulin release over prolonged periods of time or toward improving peripheral glucose utilization, because both of the latter are associated with the side effects characteristic of excess insulin action on nondesired target tissues, such as smooth muscle vesicular endothelium, which undergoes hypertrophy leading to hypertension and vascular disease.

ACKNOWLEDGMENTS

This work was supported by an award from the American Heart Association to P.H. and National Institutes of Health awards GM-071520 and DK-64166 to M.A.F. and DK-55811 to J.E.P. O.Y. was supported by a National Institute of General Medical Sciences Medical Scientist Training Program T32 training award, an individual F31 National Research Service Award from the National Institute of Diabetes and Digestive and Kidney Diseases (NIDDK), and the Turner Foundation. M.O. was supported by an individual F31 National Research Service Award from NIDDK. P.T. was supported by an NIDDK postdoctoral fellow T32 training award.

No potential conflicts of interest relevant to this article were reported.

P.H. and O.Y. researched data and wrote the article. H.Z., P.T., W.S, X.Y., S.T., and M.O. researched data. Y.K. and J.E.P. reviewed and edited the article and contributed to discussion. M.A.F. wrote the article.

The authors thank S. Vanhorn (Stony Brook University) for electron microscopy assistance, and J. Burchfield (Garvan Institute of Medical Research) and Z. Ma (Mount Sinai School of Medicine) for experimental advice.

REFERENCES

1. Muoio DM, Newgard CB. Mechanisms of disease: molecular and metabolic mechanisms of insulin resistance and beta-cell failure in type 2 diabetes. Nat Rev Mol Cell Biol 2008;9:193–205
2. Michael DJ, Ritzel RA, Haataja L, Chow RH. Pancreatic beta-cells secrete insulin in fast- and slow-release forms. Diabetes 2006;55:600–607
3. Huang CN, Chou WC, Lin LY, et al. First phase release coefficient of insulin in subjects with normal glucose tolerance on glucose infusion analyzed by computer simulation. Biosystems 2008;91:146–157
4. Li G, Rungger-Brändle E, Just I, Jonas JC, Aktories K, Wollheim CB. Effect of disruption of actin filaments by Clostridium botulinum C2 toxin on

insulin secretion in HIT-T15 cells and pancreatic islets. Mol Biol Cell 1994; 5:1199–1213
5. Li J, Luo R, Kowluru A, Li G. Novel regulation by Rac1 of glucose- and forskolin-induced insulin secretion in INS-1 beta-cells. Am J Physiol Endocrinol Metab 2004;286:E818–E827
6. Waselle L, Coppola T, Fukuda M, et al. Involvement of the Rab27 binding protein Slac2c/MyRIP in insulin exocytosis. Mol Biol Cell 2003;14:4103–4113
7. Waselle L, Gerona RR, Vitale N, Martin TF, Bader MF, Regazzi R. Role of phosphoinositide signaling in the control of insulin exocytosis. Mol Endocrinol 2005;19:3097–3106
8. Barker CJ, Leibiger IB, Leibiger B, Berggren PO. Phosphorylated inositol compounds in beta-cell stimulus-response coupling. Am J Physiol Endocrinol Metab 2002;283:E1113–E1122
9. Heath CM, Stahl PD, Barbieri MA. Lipid kinases play crucial and multiple roles in membrane trafficking and signaling. Histol Histopathol 2003;18: 989–998
10. Di Paolo G, Moskowitz HS, Gipson K, et al. Impaired PtdIns(4,5)P2 synthesis in nerve terminals produces defects in synaptic vesicle trafficking. Nature 2004;431:415–422
11. Gong LW, Di Paolo G, Diaz E, et al. Phosphatidylinositol phosphate kinase type I gamma regulates dynamics of large dense-core vesicle fusion. Proc Natl Acad Sci U S A 2005;102:5204–5209
12. Hay JC, Fisette PL, Jenkins GH, et al. ATP-dependent inositide phosphorylation required for Ca(2+)-activated secretion. Nature 1995;374:173–177
13. Grishanin RN, Kowalchyk JA, Klenchin VA, et al. CAPS acts at a prefusion step in dense-core vesicle exocytosis as a PIP2 binding protein. Neuron 2004;43:551–562
14. James DJ, Khodthong C, Kowalchyk JA, Martin TF. Phosphatidylinositol 4,5-bisphosphate regulates SNARE-dependent membrane fusion. J Cell Biol 2008;182:355–366
15. Gamper N, Reznikov V, Yamada Y, Yang J, Shapiro MS. Phosphatidylinositol [correction] 4,5-bisphosphate signals underlie receptor-specific Gq/11-mediated modulation of N-type Ca2+ channels. J Neurosci 2004; 24:10980–10992
16. Delmas P, Coste B, Gamper N, Shapiro MS. Phosphoinositide lipid second messengers: new paradigms for calcium channel modulation. Neuron 2005;47:179–182
17. Ishihara H, Wada T, Kizuki N, et al. Enhanced phosphoinositide hydrolysis via overexpression of phospholipase C beta1 or delta1 inhibits stimulus-induced insulin release in insulinoma MIN6 cells. Biochem Biophys Res Commun 1999;254:77–82
18. Lawrence JT, Birnbaum MJ. ADP-ribosylation factor 6 regulates insulin secretion through plasma membrane phosphatidylinositol 4,5-bisphosphate. Proc Natl Acad Sci U S A 2003;100:13320–13325
19. Olsen HL, Hoy M, Zhang W, et al. Phosphatidylinositol 4-kinase serves as a metabolic sensor and regulates priming of secretory granules in pancreatic beta cells. Proc Natl Acad Sci U S A 2003;100:5187–5192
20. Hammond GR, Dove SK, Nicol A, Pinxteren JA, Zicha D, Schiavo G. Elimination of plasma membrane phosphatidylinositol (4,5)-bisphosphate is required for exocytosis from mast cells. J Cell Sci 2006;119:2084–2094
21. Baukrowitz T, Schulte U, Oliver D, et al. PIP2 and PIP as determinants for ATP inhibition of KATP channels. Science 1998;282:1141–1144
22. Shyng SL, Nichols CG. Membrane phospholipid control of nucleotide sensitivity of KATP channels. Science 1998;282:1138–1141
23. Lin CW, Yan F, Shimamura S, Barg S, Shyng SL. Membrane phosphoinositides control insulin secretion through their effects on ATP-sensitive K+ channel activity. Diabetes 2005;54:2852–2858
24. Fan Z, Makielski JC. Anionic phospholipids activate ATP-sensitive potassium channels. J Biol Chem 1997;272:5388–5395
25. Zhang L, Marcu MG, Nau-Staudt K, Trifaró JM. Recombinant scinderin enhances exocytosis, an effect blocked by two scinderin-derived actin-binding peptides and PIP2. Neuron 1996;17:287–296
26. Shyng SL, Barbieri A, Gumusboga A, et al. Modulation of nucleotide sensitivity of ATP-sensitive potassium channels by phosphatidylinositol-4-phosphate 5-kinase. Proc Natl Acad Sci U S A 2000;97:937–941
27. Vicogne J, Vollenweider D, Smith JR, Huang P, Frohman MA, Pessin JE. Asymmetric phospholipid distribution drives in vitro reconstituted SNARE-dependent membrane fusion. Proc Natl Acad Sci U S A 2006;103: 14761–14766
28. Thore S, Wuttke A, Tengholm A. Rapid turnover of phosphatidylinositol-4,5-bisphosphate in insulin-secreting cells mediated by Ca2+ and the ATP-to-ADP ratio. Diabetes 2007;56:818–826
29. Hilpelä P, Vartiainen MK, Lappalainen P. Regulation of the actin cytoskeleton by PI(4,5)P2 and PI(3,4,5)P3. Curr Top Microbiol Immunol 2004; 282:117–163
30. Hao M, Bogan JS. Cholesterol regulates glucose-stimulated insulin secretion through phosphatidylinositol 4,5-bisphosphate. J Biol Chem 2009;284: 29489–29498
31. Vitale N, Caumont AS, Chasserot-Golaz S, et al. Phospholipase D1: a key factor for the exocytotic machinery in neuroendocrine cells. EMBO J 2001; 20:2424–2434
32. Thurmond DC, Gonelle-Gispert C, Furukawa M, Halban PA, Pessin JE. Glucose-stimulated insulin secretion is coupled to the interaction of actin with the t-SNARE (target membrane soluble N-ethylmaleimide-sensitive factor attachment protein receptor protein) complex. Mol Endocrinol 2003;17:732–742
33. Jewell JL, Luo W, Oh E, Wang Z, Thurmond DC. Filamentous actin regulates insulin exocytosis through direct interaction with Syntaxin 4. J Biol Chem 2008;283:10716–10726
34. Olofsson CS, Håkansson J, Salehi A, et al. Impaired insulin exocytosis in neural cell adhesion molecule-/- mice due to defective reorganization of the submembrane F-actin network. Endocrinology 2009;150:3067–3075
35. Bittner MA, Holz RW. Phosphatidylinositol-4,5-bisphosphate: actin dynamics and the regulation of ATP-dependent and -independent secretion. Mol Pharmacol 2005;67:1089–1098
36. Sasaki J, Sasaki T, Yamazaki M, et al. Regulation of anaphylactic responses by phosphatidylinositol phosphate kinase type I alpha. J Exp Med 2005; 201:859–870
37. Zhang J, Luo R, Wu H, Wei S, Han W, Li G. Role of type Ialpha phosphatidylinositol-4-phosphate 5-kinase in insulin secretion, glucose metabolism, and membrane potential in INS-1 beta-cells. Endocrinology 2009;150:2127–2135
38. Morioka T, Asilmaz E, Hu J, et al. Disruption of leptin receptor expression in the pancreas directly affects beta cell growth and function in mice. J Clin Invest 2007;117:2860–2868
39. Fearnside JF, Dumas ME, Rothwell AR, et al. Phylometabonomic patterns of adaptation to high fat diet feeding in inbred mice. PLoS One 2008;3: e1668
40. Oude Weernink PA, Schmidt M, Jakobs KH. Regulation and cellular roles of phosphoinositide 5-kinases. Eur J Pharmacol 2004;500:87–99
41. Gomi H, Mizutani S, Kasai K, Itohara S, Izumi T. Granuphilin molecularly docks insulin granules to the fusion machinery. J Cell Biol 2005;171:99–109
42. Oh E, Thurmond DC. Munc18c depletion selectively impairs the sustained phase of insulin release. Diabetes 2009;58:1165–1174
43. Ivarsson R, Jing X, Waselle L, Regazzi R, Renström E. Myosin 5a controls insulin granule recruitment during late-phase secretion. Traffic 2005;6: 1027–1035
44. Aoyagi K, Sugaya T, Umeda M, Yamamoto S, Terakawa S, Takahashi M. The activation of exocytotic sites by the formation of phosphatidylinositol 4,5-bisphosphate microdomains at yntaxin clusters. J Biol Chem 2005;280: 17346–17352
45. Laux T, Fukami K, Thelen M, Golub T, Frey D, Caroni P. GAP43, MARCKS, and CAP23 modulate PI(4,5)P(2) at plasmalemmal rafts, and regulate cell cortex actin dynamics through a common mechanism. J Cell Biol 2000;149: 1455–1472